

Momentum-Dependent Charge Transfer Excitations in $\text{Sr}_2\text{CuO}_2\text{Cl}_2$ Angle-Resolved Electron Energy Loss Spectroscopy

Y. Y. Wang,¹ F. C. Zhang,^{2,3} V. P. Dravid,¹ K. K. Ng,² M. V. Klein,⁴ S. E. Schnatterly,⁵ and L. L. Miller⁶

¹*Department of Materials Science and Engineering, Northwestern University, Evanston, Illinois 60208*
²*and Science and Technology Center for Superconductivity, Northwestern University, Evanston, Illinois 60208*

²*Department of Physics, University of Cincinnati, Cincinnati, Ohio 45221*

³*Department of Physics, Hong Kong University of Science and Technology, Clear Water Bay, Kowloon, Hong Kong*

⁴*Department of Physics, Science and Technology Center for Superconductivity, University of Illinois, Urbana, Illinois 61801*

⁵*Department of Physics, University of Virginia, Charlottesville, Virginia 22901*

⁶*Ames Laboratory, Iowa State University, Ames, Iowa 50011*

(Received 13 November 1995; revised manuscript received 3 June 1996)

Electron-hole pair excitations in the insulating cuprates $\text{Sr}_2\text{CuO}_2\text{Cl}_2$ were investigated by angle-resolved electron energy loss spectroscopy. The optically allowed and optically forbidden transitions were observed to be strongly anisotropic in the Cu-O_2 plane. The former show a large energy dispersion ~ 1.5 eV along [110], and the latter appear at a higher energy position (~ 4.5 eV) only along [100], but not along [110]. We interpret these results as transitions involving excitons. A small exciton model is examined to explain both the observed features. [S0031-9007(96)01069-1]

PACS numbers: 71.35.Cc, 74.72.Jt

The electronic structure of the cuprate superconductors has been under intense investigation in recent years in hope of revealing clues about the mechanism of high T_C superconductivity. While the superconductivity occurs in the doped materials, it is of primary importance to understand the electronic structure of the parent compounds.

Measurements of the optical dielectric constant on the parent insulator reveal a well-defined peak in its imaginary part, ϵ_2 , at 1.6–2.0 eV, which measures the charge transfer band gap with excitonic correction, followed by a weak, nonuniversal absorption at 1 eV higher energy [1]. Raman scattering experiments provide additional information. The two magnon Raman band at 0.4 eV energy shift shows a strong enhancement in $\text{YBa}_2\text{Cu}_3\text{O}_{6.1}$ when the exciting laser light approaches 3.1 eV, which is 1.3 eV above the conductivity peak [1]. Similar results were obtained from $\text{Sr}_2\text{CuO}_2\text{Cl}_2$ [2]. Optical absorption probes the dipole allowed electron-hole excitations with an essentially zero total wave vector \vec{q} . Nondipole allowed $q \sim 0$ excitations have been studied in the insulating cuprates through the use of large frequency shift Raman scattering with an ultraviolet laser [3]. Angle-resolved electron energy loss spectroscopy (EELS) probes finite \vec{q} excitations. In the EELS experiment, the differential cross section is directly related to the imaginary part of the inverse longitudinal dielectric function $\epsilon(\vec{q}, \omega)$ by $d^2\sigma/(dE d\Omega) \sim q^{-2} \text{Im}[-1/\epsilon(\vec{q}, \omega)]$. At very small q , the EELS measures the same excitations as the optical spectroscopy. At finite \vec{q} , EELS can be used to probe the dispersion of the excitation and study optically forbidden transitions [4–8].

In the present study, we have employed momentum-transfer resolved EELS to investigate the dispersion of the valence band excitations in $\text{Sr}_2\text{CuO}_2\text{Cl}_2$. For the first time, we report an optically forbidden transition (at

~ 4.5 eV) and the dispersion of the optically allowed transition, both of which are strongly anisotropic. The optically allowed excitation is found to have a large dispersion range of ~ 1.5 eV. This is remarkable in view of the narrow dispersion width 0.35 eV for a single hole in the same compound observed in the recent photoemission experiment [9]. Given the latter as a fact, the pronounced large dispersion observed in the EELS is difficult to account for within a usual interband transition picture. Here we shall provide an exciton model for the cuprate insulator, which naturally gives a large dispersion in the antiferromagnetic (AF) spin background and can also explain the anisotropy in the optically forbidden transition in the EELS.

Crystals for this work were grown from powders using a self-flux technique described in Ref. [10]. The final product of $\text{Sr}_2\text{CuO}_2\text{Cl}_2$ single crystals is a lamellar crystal which is hygroscopic. Transmission electron microscopy (TEM) specimens were fresh prepared by cleaving. The EELS data were obtained using a cold field emission TEM (Hitachi HF-2000) equipped with a Gatan 666 parallel electron energy loss spectrometer with the sample cooled to -100 °C. The peak width of the unscattered beam is ~ 0.5 eV. The zero loss peak was removed after fitting it to an asymmetric Lorentzian function [11]. Multiple scattering up to the fifth order was removed by using the standard f -sum rule procedure [12].

Figures 1(a) and 1(b) show the EELS spectrum at different momentum, \vec{q} , for $\text{Sr}_2\text{CuO}_2\text{Cl}_2$ along [100] and [110], respectively. There is an optically allowed transition in both directions, whose position is at 2.8 eV for small q , corresponding to the 2 eV excitation observed in optical spectroscopy [13–15]. With increasing q along [100], a broad transition at about 4.5 eV gradually appears. As q increases, the position of the optically

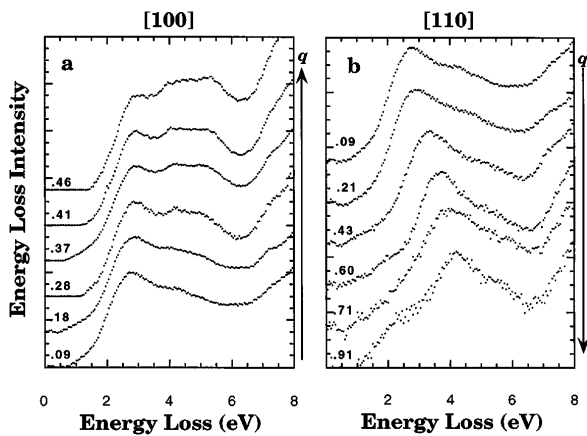


FIG. 1. Electron energy loss spectra of $\text{Sr}_2\text{CuO}_2\text{Cl}_2$ along [100] (a) and [110] (b) with different momentum transfers, given by the inserted numbers (\AA^{-1}). All intensities are in arbitrary units.

allowed transition along [110] disperses systematically towards higher energy by about 1.5 eV, while the energy position along [100] is less dispersive. This indicates that the dipole allowed transition becomes anisotropic at finite \vec{q} in the CuO_2 plane and that the bandwidth of the excitation is large.

We have also measured the intensity of the optically allowed transition relative to the other valence excitations in the loss function. As q increases, the intensity decreases rapidly along [100], while it changes little along [110]. This indicates that the oscillator strength of the dipole allowed transition is also anisotropic.

Another important feature is the optically forbidden transition located at 4.5 eV, at finite \vec{q} . The transition is strongly anisotropic, appearing along [100], but not along [110]. This implies a certain symmetry in the excitations.

To gain more insight, we carried out the Kramers-Kronig analysis to extract the excitation spectrum, or $\epsilon(\vec{q}, \omega)$, from the EELS data. We used $\epsilon(\vec{q}, \omega = 0) \approx \epsilon_0 \equiv (q = 0, \omega = 0)$, where $\epsilon_0 = 4.83$ was obtained from previous optical measurements on this material [13,14]. In Fig. 2 we show the resultant dispersion and the peak intensity of the optically allowed excitation, or the peak position and the weight of ϵ_2 , respectively, as functions of \vec{q} . The transition peak position at 2.8 eV for small q in the EELS is shifted to 2.4 eV in ϵ_2 [16]. The optical forbidden transition centered at ~ 4.5 eV in the loss function remains at the same energy position in ϵ_2 . The dispersion of the 2.4 eV excitation in the dielectric function along [110] is similar to that in the EELS, but along [100] the dispersion is substantially larger than in the loss function. However, the excitation dispersion remains anisotropic along the different orientations. The oscillator strength of the optical allowed excitation declines quickly along [100], while it remains almost unchanged along [110].

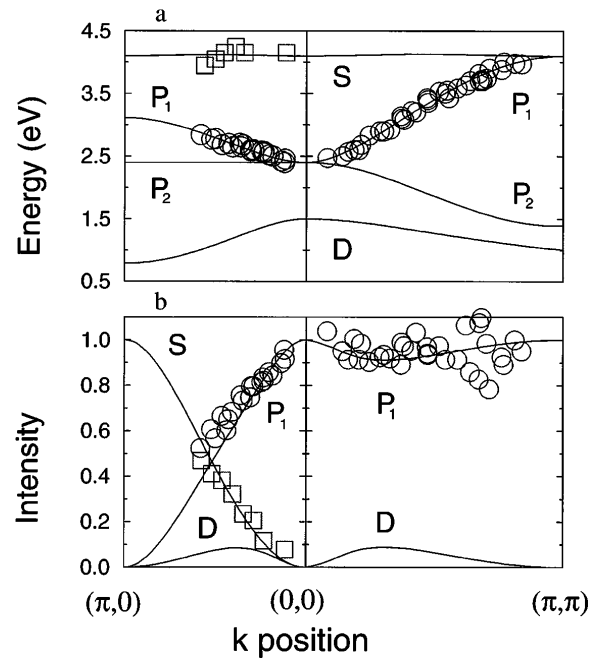


FIG. 2. The dispersion (a) and the intensity (b) along [100] and [110] directions. The circles are the optically allowed transitions and the squares are the optically forbidden transitions obtained from the EELS after the Kramers-Kronig analysis. The solid lines are the theoretical results for the parameters $t_1 = 0.4$, $t_2 = 0.126$, $t_3 = 0.85$, and $t_4 = 0.65$ eV. The energy for the P mode at $k = 0$ is set equal to the optically allowed transition in the EELS, which also corresponds to the optical gap.

It is interesting to note that the oscillator strength of the optically forbidden excitation at ~ 4.5 eV compensates the strength of the optically allowed excitation. As the scattering angle increases along [100], the strength of the forbidden excitation grows, and the strength of the allowed one decreases. However, along [110], there is no forbidden excitation, and the intensity of the optical branch remains unchanged. This compensation indicates that these two excitations are closely related to each other.

The most interesting result in the EELS is the large dispersion of ~ 1.5 eV for the dipole allowed transition. This may be surprising because of the much narrower dispersion for the single hole observed in the photoemission experiment [9]. The undoped system is an AF. A hole moving in the AF spin background is strongly affected by the spins, so that the coherent bandwidth is small. The same is expected for a single electron ($\text{Cu } 3d^{10}$) state. If the excitation were from the transition between the independent hole and electron band (continuum), we would have a much smaller dispersion (~ 0.3 eV) than the one observed by our experiment (~ 1.5 eV) [17]. Furthermore, according to the angle-resolved photoemission experiment [9], the top of the hole band is located at $(\pm\pi/2, \pm\pi/2)$. As expected, the bottom of the electron band would also be at $(\pm\pi/2, \pm\pi/2)$. Therefore, according to the

continuum picture, the interband transition threshold for $\vec{q} = (\pi, \pi)$ and $\vec{q} = 0$ would be the same, which is inconsistent with the observed monotonic increase of the dispersion along [110] extended to near the zone boundary in our experiment.

In a conventional semiconductor, in addition to the electron-hole ($e-h$) continuum, pairs of electron and hole (excitons) also contribute to the EELS. The exciton spectrum is below the $e-h$ continuum, and its bandwidth is narrower than that of the electron or hole separately [18]. The undoped cuprate is a Mott insulator, and the narrow dispersion of a hole or electron is due to the largely incoherent motion in the spin background. In this case, a spin singlet electron hole pair may move rather freely without disturbing the spins, giving a larger dispersion in the EELS. We shall examine an exciton model for the cuprate insulator to show that the EELS dispersion can be indeed large and that the anisotropic optically forbidden transition is due to the intensity transfer of the exciton states.

Let us consider an undoped CuO_2 plane. The ground state is a spin-1/2 AF of Cu^{2+} with one hole at each Cu site [19]. The low energy charge transition is a hole transferred from Cu $3d_{x^2-y^2}$ to O $2p\sigma$ states. Because of the strong hybridization, a square of O hole will bind to the central Cu^{2+} to form a spin singlet [20], or a formal Cu^{3+} . We introduce an attractive Coulomb interaction $-V$ between the quasiparticle (Cu^+) and the quasihole (formal Cu^{3+}). For simplicity we consider the effective hoppings of the Cu^+ or Cu^{3+} to be small and include the nearest neighbor (nn) Coulomb attraction only. Namely, we study the small exciton limit as illustrated in Fig. 3. For a given site of Cu^+ , there are four different quasiholes in space due to the fourfold rotational symmetry of the CuO_2 plane. We can construct four local symmetry states with s , $d_{x^2-y^2}$, and two types of p waves according to their relative phases [21]. We now consider the exciton motion, primarily due to the nn Cu-O and the O-O direct hoppings. Because each exciton involves a pair of neighboring Cu sites, both are spinless and the exciton can move through the lattice without disturbing the spins, similar to a pair of bound nn holes. When the exciton moves in a finite \vec{q} , the different local symmetry states will mix with each other. For each \vec{q} , there are four eigenmodes denoted by S , D , P_1 , and P_2 according to their local symmetries in the limit $q \rightarrow 0$, where P_1 and P_2 are the dipole active and dipole inactive modes, respectively. The dispersion and the symmetry of the exciton modes determine the EELS in our theory.

In what follows, we briefly summarize the basic results obtained from a more detailed mathematical formalism [22]. We parametrize the exciton hopping by four integrals, which are found to be the most significant based on a perturbation theory in the atomic limit. Let us denote the exciton hopping integral for $\tau(\vec{R}) \rightarrow \tau'(\vec{R}')$ to be $t_{\tau\tau'}(\vec{R} - \vec{R}')$, where \vec{R} is the position of the Cu^+ and τ is

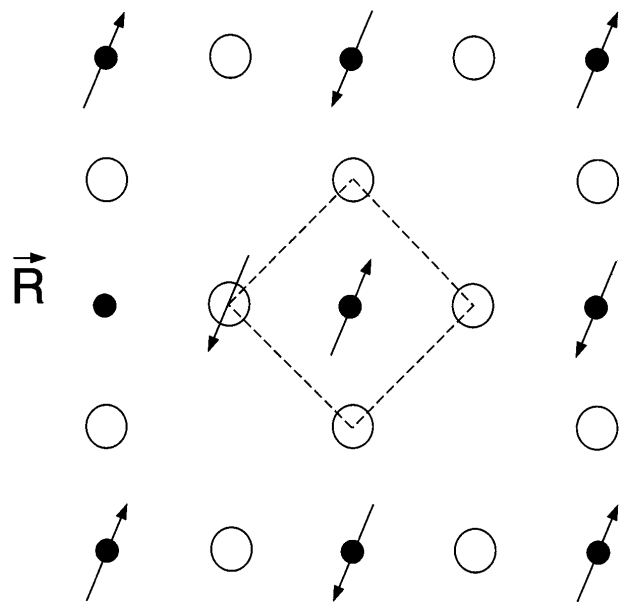


FIG. 3. The structure of a local exciton in CuO_2 plane. The open circles represent O atoms, solid circles represent Cu atoms, the arrows represent spins of holes. The quasiparticle (Cu^+) is at the vacant Cu site \vec{R} , and the quasihole is on the square of O atoms and forms a spin singlet with the central Cu hole.

the position of the formal Cu^{3+} relative to the Cu^+ . The important hopping integrals are $t_1 \equiv t_{\hat{x},\hat{y}}(0)$, $t_2 \equiv t_{\hat{x},\hat{y}}(\hat{x})$, $-t_3 \equiv t_{\hat{x},-\hat{x}}(\hat{x})$, and $t_4 \equiv t_{\hat{x},\hat{x}}(0)$. $t_3 \sim t_{pd}^2/\epsilon_p$, with t_{pd} the Cu-O hopping and ϵ_p the atomic energy difference between the Cu and O hole states. t_3 is of order of hole hopping integral in the doped Cu oxides. The dynamics of the exciton can be described by a tight-binding Hamiltonian, which can be solved. The calculated dispersions are plotted in Fig. 2(a) for a set of parameters to fit the EELS data. The S mode has the highest energy, while the D mode has the lowest. At $k = 0$, both S and D modes are optically forbidden because of the d symmetry of the Cu hole. P_1 is optically active, and the charge transfer gap is $\Delta = \epsilon_p - E_s - V + t_4 - t_3$, E_s is the hybridization energy of the Cu-O singlet. The optical gap observed in the experiment is identified as Δ , and a sharp peak at Δ is expected. This is consistent with the optical conductivity spectra [15] for $\text{Sr}_2\text{CuO}_2\text{Cl}_2$, where a fairly sharp profile of the absorption peak has been observed. The exciton dispersions are anisotropic. The energy of the P_1 mode is monotonic along the [110] direction, and the dispersion width is given by $2t_3$, a large energy scale.

The EELS intensity of the exciton is given by $I \sim q^{-2} |\langle \Psi_{\text{ex}} | e^{i\vec{q}\cdot\vec{r}} | \text{GS} \rangle|^2$, where $|\Psi_{\text{ex}}\rangle$ and $|\text{GS}\rangle$ are the exciton and ground states, respectively. We use the dipole approximation to calculate the intensity, so that $I = I_0 |\langle \Psi_{\text{ex}} | p_1 \rangle|^2$, where I_0 is the dipole active intensity of the P_1 mode at $q = 0$, and $|p_1\rangle$ is the P_1 state in the limit $\vec{q} \rightarrow 0$. It is the overlap amplitude between the exciton state and the dipole mode p_1 which determines

the dipole active intensity in the EELS. The calculated intensities of the excitons are plotted in Fig. 2(b). Along [100], the intensity of the P_1 mode is transferred to the S mode as q increases, which explains the gradual appearance of the broad forbidden transition at 4.5 eV [23]. Along the [110] direction, the intensity of the P_1 mode is quite flat, and the S mode remains dipole inactive. It can be further shown that along [110] the S mode does not couple to p_1 , and the intensity vanishes up to quadrupole order [22]. The strong anisotropy is due to the fourfold lattice symmetry. These features are in excellent agreement with the EELS data.

The D mode exciton, expected from the theory, is another optically forbidden state. The current EELS does not reveal this mode, probably due to the limit of the experiment resolution. Further spectroscopy works are needed to verify this d -wave-like state. This mode can be active in the phonon-assisted optical process, and should be observable in luminescence experiments. A recent optical absorption measurement indicates a very weak absorption state at about 0.5 eV in the undoped cuprates [24]. The d -symmetry state is an alternative to the magnon state or crystal field exciton [24,25] proposed previously for this weak absorption where the phonons could be involved.

We now briefly comment on the relation to the e - h continuum, which starts at $\Delta_{e-h} = \epsilon_p - E_s + E_{\text{kin}}$, where $E_{\text{kin}} < 0$ is the kinetic energy of the independent Cu^+ and Cu^{3+} . In our model, E_{kin} is treated perturbatively. For the cuprates, $-E_{\text{kin}}$ is $\sim 1-2$ eV, but there is no direct experimental data for V . The large dispersion of the EELS reported here may be viewed as an indication that V is not very small for the undoped materials. If $V \sim -E_{\text{kin}}$, which may be the case for the cuprates, a complete exciton theory should also include its spatial extension, but some features examined here should remain. In this case, we expect the e - h continuum to start above the $q = 0$ P_1 mode, and the exciton spectra extend into the e - h continuum due to the large spectral dispersion. The states above the e - h continuum will then be damped, but can exist as resonant states contributing to the EELS. This feature is very different from the usual semiconductors, and is due to the AF spin background. Since the contributions to the EELS from the e - h continuum have much less \vec{q} dependence, we argue that the excitons be the dominant source of the \vec{q} dependence in the EELS.

In summary, we reported \vec{q} -resolved EELS in $\text{Sr}_2\text{CuO}_2\text{Cl}_2$ and observed a large energy dispersion of 1.5 eV of the optically allowed transition and a very anisotropic optically forbidden transition at a higher energy. We have presented a small exciton model, in which the exciton moves almost freely in the AF spin

background, to explain both features of the EELS. While more sophisticated theories are needed for a complete description (such as the lifetime of the excitons and the interaction between the excitons and the e - h continuum), our model contains interesting ingredients for explaining the seemingly unusual EELS data.

We would like to thank N. Bulut, P. D. Han, K. Zhang, T. K. Ng, S. Haas, and, in particular, T. M. Rice for many useful discussions. The research is supported in part by NSF-DMR-91-20000 through the Science and Technology Center for Superconductivity and by the U.S. Department of Energy through Ames Laboratory under Contract No. W-7405-Eng-82. One of us (K. K. N.) wishes to acknowledge the URC at University of Cincinnati for the summer fellowship.

-
- [1] S. L. Cooper *et al.*, Phys. Rev. B **47**, 8233 (1993).
 - [2] G. Blumberg, Phys. Rev. B **53**, 11 930 (1996).
 - [3] D. Salamon *et al.*, Phys. Rev. B **51**, 6617 (1995).
 - [4] Y. Y. Wang *et al.*, Phys. Rev. Lett. **75**, 2546 (1995).
 - [5] N. Nucker *et al.*, Phys. Rev. B **44**, 7155 (1991).
 - [6] J. J. Ritsko *et al.*, Phys. Rev. Lett. **36**, 210 (1976).
 - [7] S. E. Schnatterly, in *Solid State Physics* (Academic Press, New York, 1979), Vol. 14.
 - [8] H. Raether, *Excitation of Plasma and Interband Transitions by Electrons* (Springer-Verlag, Berlin, 1980).
 - [9] B. O. Wells *et al.*, Phys. Rev. Lett. **74**, 964 (1995).
 - [10] L. L. Miller *et al.*, Phys. Rev. B **41**, 1921 (1990).
 - [11] Y. Y. Wang *et al.*, Ultramicroscopy **33**, 151 (1990).
 - [12] Y. Y. Wang, Ultramicroscopy **33**, 151 (1990).
 - [13] P. Abbemonte, J. Graybeal, D. Tanner, and A. Zibold (private communication).
 - [14] S. Tajima *et al.*, Physica (Amsterdam) **168C**, 117 (1990).
 - [15] Y. Tokura *et al.*, Phys. Rev. B **41**, 11 657 (1990).
 - [16] The energy difference between the EELS and the optical spectrum is most likely due to the instrumental broadening.
 - [17] The incoherent states in both valence and conduction bands are of large energy range, but their contributions to the transition are expected to be weakly q dependent because of the incoherent nature.
 - [18] D. C. Mattis and J. P. Gallinar, Phys. Rev. Lett. **53**, 1391 (1984).
 - [19] D. Vaknin *et al.*, Phys. Rev. B **41**, 1926 (1990).
 - [20] F. C. Zhang and T. M. Rice, Phys. Rev. B **37**, 3759 (1988).
 - [21] M. J. Rice and Y. R. Wang, Phys. Rev. B **36**, 8794 (1987).
 - [22] F. C. Zhang *et al.* (unpublished).
 - [23] Close examination indicates two features: one at 4.1 eV and one at 4.9 eV. We tentatively assign the lower one to be the S mode of the exciton discussed in the paper.
 - [24] J. D. Perkins *et al.*, Phys. Rev. Lett. **71**, 1621 (1993).
 - [25] J. Lorentzana and G. A. Sawatzky, Phys. Rev. Lett. **74**, 1867 (1995).